

# Alginate-Based Hydrogels with Amniotic Membrane Stem Cells for Wound Dressing Application

Nurul Fitriani<sup>1,2</sup>, Gofarana Wilar<sup>3</sup>, Angga Cipta Narsa<sup>2</sup>, Khaled M Elamin<sup>4</sup>, Nasrul Wathoni<sup>1</sup>

<sup>1</sup>Department of Pharmaceutics and Pharmaceutical Technology, Faculty of Pharmacy, Universitas Padjadjaran, Sumedang, 45363, Indonesia;

<sup>2</sup>Pharmaceutical Research and Development Laboratory of FARMAKA TROPIS, Faculty of Pharmacy, Universitas Mulawarman, Samarinda, 75119, Indonesia; <sup>3</sup>Department of Pharmacology and Clinical Pharmacy, Faculty of Pharmacy, Universitas Padjadjaran, Jatinangor, 45363, Indonesia; <sup>4</sup>Graduate School of Pharmaceutical Sciences, Kumamoto University, Chuo-ku, Kumamoto, 862-0973, Japan

Correspondence: Nasrul Wathoni, Department of Pharmaceutics and Pharmaceutical Technology, Faculty of Pharmacy, Universitas Padjadjaran, Sumedang, 45363, Indonesia, Tel/Fax +6222 842 888888, Email nasrul@unpad.ac.id

**Objective:** Chronic wounds are a common clinical problem that necessitate the exploration of novel regenerative therapies. We report a method to investigate the in vitro wound healing capacity of an innovative biomaterial, which is based on amniotic membrane-derived stem cells (AMSCs) embedded in an alginate hydrogel matrix. The aim of this study was to prepare an sodium alginate-based hydrogel, cross-linked calcium chloride (CaCl<sub>2</sub>) with the active ingredient AMSC (AMSC/Alg-H) and to evaluate its in vitro effectiveness for wound closure.

**Methods:** This hydrogel preparation involved combining sterile solutions of AMSC, sodium alginate, and CaCl<sub>2</sub>, followed by rinsing with serum-free media. The cells were cultured in different 6-well plates, namely sodium alginate, calcium chloride, AMSC, Alg-H, and AMSC/Alg-H, in complete medium with 10% FBS. The hydrogel was successfully formulated, as confirmed by characterization techniques including Scanning Electron Microscopy (SEM), Fourier Transform Infrared (FTIR) spectroscopy, Differential Scanning Calorimetry (DSC), Cytotoxicity Studies, TGF-β1 Level Measurement by ELISA, and Cell Scratch Wound Assay.

**Results:** Cryo-EM characterization of the Alg-H preparation successfully demonstrated the encapsulation of MSCs. FTIR and DSC analyses indicate that crosslinking transpires in Alg-H encapsulating AMSC. The AMSC/Alg-H preparation showed no significant difference in toxicity compared to HaCaT cells ( $p < 0.05$ ), indicating it was not toxic to HaCaT cells. Furthermore, in the scratch wound assay test at 24 hours, the AMSC/Alg-H preparation achieved 100% wound closure, outperforming both AMSC and Alg-H alone. In vitro assessment revealed that AMSC/Alg-H significantly enhanced key wound healing processes, including cell proliferation and migration, compared to Alg-H.

**Conclusion:** Our study demonstrated the promising potential of AMSC/Alg-H as an enhanced regenerative therapy for in vitro wound healing. AMSC/Alg-H was able to maintain the viability of AMSCs and facilitate the formation of tissue-like structures.

**Keywords:** AMSC, alginate, hydrogel, wound healing

## Introduction

Stem cell research holds significant promise for the development of therapies for severe illnesses and traumas. Regenerative therapy involves the use of living cells or stem cells to repair, replace, or restore the normal function of damaged tissues and organs.<sup>1,2</sup>

Amniotic membrane stem cells (AMSCs) are a type of Mesenchymal Stem Cell (MSC) that include various growth factors, such as epidermal growth factor (EGF), basic fibroblast growth factor (bFGF), keratinocyte growth factor (KGF), vascular EGF (VEGF), transforming growth factors (TGFs), and nerve growth factors (NGF), and chemokines. These factors are essential in the process of wound healing, regardless of whether the wounds are acute or chronic.<sup>3</sup> AMSCs promote faster healing and anti-inflammatory effects, making them safe and compatible with human donors. They are less likely to provoke an immune response than other types of grafts.<sup>4</sup> Additionally, they possess inherent antimicrobial

properties that provide protection against common wound infections. They also have antimicrobial properties, protecting against infections. The unique biological properties, safety profile, practical advantages, and demonstrated clinical efficacy of AMSCs make them a superior choice for wound dressings compared to other stem cell types.<sup>5–7</sup>

Hydrogels are increasingly preferred because of their biocompatibility, flexible physical properties, structural resemblance to native extracellular matrices, and the capacity to promote cellular adhesion and growth. Hydrogels create a 3D setting for cell growth, allowing for a cell structure and function that are not achievable in 2D settings. The purpose of utilizing a hydrogel-based matrix is to replicate the natural cellular environment in place of an extracellular matrix, offering essential sites for cell adhesion, feeding, and exposure to paracrine signals.<sup>8,9</sup> Hydrogels are becoming increasingly popular because they are compatible with living organisms, have flexible physical characteristics, resemble the structure of natural extracellular matrices, and enhance the attachment and proliferation of cells.

Prior research has employed polymers in tissue engineering to enhance wound healing results. Micronized amniotic membrane (mAM) is a polymer that improves the survival and proliferation of mesenchymal stem cells (MSCs) in vitro and promotes accelerated healing of burn wounds in vivo.<sup>10</sup> Furthermore, collagen in conjunction with AMSCs facilitates cell adhesion, proliferation, and differentiation, thereby augmenting the regenerative capabilities of AMSCs.<sup>11</sup> Chitosan exhibits antibacterial and biocompatibility properties, indicating its potential to enhance wound healing by promoting cell migration and proliferation.<sup>12</sup>

Alginate is a natural polymer used to create hydrogels. Alginate is an appealing substance for wound dressings owing to its hydrophilicity, excellent biocompatibility, and high fluid absorption capacity. Alginate can trigger macrophages and prompt monocytes to generate interleukin-6 (IL-6) and tumor necrosis factor (TNF- $\alpha$ ) to accelerate the healing process of chronic wounds.<sup>13</sup> Studies indicate that alginate-hyaluronic acid hydrogels increase the proliferation and maturation of human mesenchymal stem cells (hMSCs) in a three-dimensional culture system, achieving a survival rate of 77.36% over 14 days.<sup>14</sup> Alginate hydrogel capsules demonstrated the ability to maintain cell viability and functionality, making them a viable choice for a delivery route for adipose tissue-derived mesenchymal stem cells.<sup>15</sup> Alginate-based materials have been investigated for their improved wound healing capabilities, with additions like nanoparticles augmenting antibacterial characteristics while preserving cell viability.<sup>16</sup> Moreover, alginate-based polymers loaded with silver nanoparticles (AgNPs) have antimicrobial characteristics and enhance wound closure rates.<sup>17</sup> A study demonstrated that alginate hydrogel containing hMSC secretome and extracellular matrix components can augment cell migration and proliferation, as well as collagen synthesis, both in vitro and in vivo, resulting in enhanced healing, neovascularization, and increased epidermal thickness.<sup>18</sup> Moreover, the alginate-based hydrogel integrated with carboxymethyl cellulose demonstrated a substantial decrease in wound area over time, suggesting its efficacy in skin regeneration.<sup>19</sup> Alginate's mechanical strength and biocompatibility render it an optimal selection for regenerative medicine applications employing AMSC therapy. Alginate was cross-linked using calcium chloride (CaCl<sub>2</sub>) to form a hydrogel. When alginate interacts with divalent cations such as calcium (Ca<sup>2+</sup>), it undergoes a chemical reaction and produces a gel structure. When cross-linked with CaCl<sub>2</sub>, it produces a three-dimensional structure that can transport drugs and consistently release them into the injured area. Alginate's biocompatibility, capacity to preserve stem cell viability, and facilitation of improved cellular functioning render it an exemplary prospect for regenerative medicine applications utilizing AMSC therapy. These findings highlight the necessity of creating efficient biomaterials that can enhance stem cell functionality in wound healing scenarios.<sup>20</sup>

This work proposes the use of an alginate-based hydrogel as a delivery vehicle for Amniotic Membrane Stem Cells with the aim of facilitating the wound healing process. This study focuses on the chemical and biological characteristics of AMSC/Alg-H. The aim of this study was to create a hydrogel (Alg-H) with the active ingredient AMSC for wound healing.

## Material and Methods

### Materials

Amniotic membrane stem cells from the Stem Cell Research and Development Center (Surabaya, East Java, Indonesia), sodium alginate from Himedia (Kennett Square, USA), calcium chloride, fetal bovine serum (FBS), and Elisa Kit from

Sigma-Aldrich (St. Louis, MO, USA), HaCaT Cells from the American Type Culture Collection (Manassas, VA, USA), and Dulbecco's Modified Eagle Medium from Mediatech (Manassas, VA, USA) was used.

### Preparation of AMSC/Alg-H

A (1 mL) was thoroughly combined with 2 mL of a sterile sodium alginate (SA) solution at a concentration of 150 mM (pH 7.4). The final SA concentration in the mixture was 100 mM. This was performed in six-well plates. A 1 mL solution of sterile  $\text{CaCl}_2$  with a concentration of 150 mM and a pH of 7.4 was used to harden the AMSC-alginate complex (Table 1). This process took 2–3 minutes to complete. The resulting gel was washed several times with a serum-free medium. The preparation of sterile SA and sterile  $\text{CaCl}_2$  solution was carried out in LAF. SA and  $\text{CaCl}_2$  powder was dissolved in distilled water and then filtered using a membrane filter with pores of 0.22  $\mu\text{m}$  twice. The control group consisted of an equivalent number of cells that were cultivated on a separate 6-well plate, but were not treated with alginate. AMSC, Alg-H, and AMSC/Alg-H were grown in 10% FBS-complete medium and incubated at 37 °C in the same environment. The medium was replaced every three days, and the supernatant from each well was collected.<sup>21</sup>

### Morphology Studies

To prepare AMSC, Alg-H, and AMSC/Alg-H for analysis, they were frozen in vitreous ice and then placed into the cryogenic sample holder of a FTALOS 200C cryo-electron microscope (Hillsboro, Oregon, USA). Subsequently, the samples were cooled to the desired temperature. The imaging conditions were optimized to achieve the best contrast and resolution. Images or videos of the frozen samples were captured using a microscope imaging detector. Specialized software programs were used for the image processing and 3D reconstruction.<sup>22–24</sup>

### Fourier-Transform Infrared Spectroscopy Analysis (FTIR)

The chemical interactions of AMSC, Alg-H, and AMSC/Alg-H were investigated using a Fourier-transform infrared spectrophotometer (FTIR) (Thermo Fisher, Waltham, MA, USA) and measured at 4000–400  $\text{cm}^{-1}$ . To analyze the AMSC, Alg-H, and AMSC/Alg-H samples, the samples were placed between two NaCl plates or within a liquid sample cell. The FTIR spectrometer was activated, a background scan was performed to acquire a reference spectrum, and the sample was placed in the sample compartment. Execute the necessary number of scans and gather the data to assemble the sample spectrum.<sup>25–27</sup>

### Differential Scanning Calorimetry Analysis (DSC)

The thermal properties of the composites prepared with AMSC, Alg-H, and AMSC/Alg-H were evaluated by differential scanning calorimetry (DSC) using a Perkin Elmer DSC 6000 instrument (Massachusetts, USA). Sample Preparation the AMSC, Alg-H and AMSC/Alg-H were subjected to thermal analysis in the temperature range of 25°C –300°C at a heating rate of 10°C/min under continuous flow nitrogen gas at a rate of 50 mL/min.<sup>25,28</sup>

### Preparation of HaCaT Cell

HaCaT cells were cultivated in Dulbecco's Modified Eagle's Medium (DMEM) augmented with Penicillin-Streptomycin antibiotics (10 mg/mL) and fetal bovine serum (FBS). HaCaT cells must be at least 80% confluent for usage. The media in the flask is subsequently removed, followed by rinsing the cells twice with 10 mL of PBS. 3 mL of trypsin-EDTA solution is administered and thereafter incubated for five minutes to facilitate the dispersion of the cell layer (under an inverted microscope, the cells will appear to be suspended). The cells and media are subjected to centrifugation at 1500 rpm for 5 minutes. The supernatant is removed, and the cell pellet is re-suspended in fresh complete media.

**Table 1** AMSC Formulation

Formulation	AMSC (mL)	Alg (mL)	$\text{CaCl}_2$ (mL)
AMSC	1	–	–
Alg-H	–	2	1
AMSC/Alg-H	1	2	1

## Cytotoxicity Studies

HaCaT cells were seeded at a density of 100,000 cells/200  $\mu$ L per well in 96-well plates and incubated for 48 hours at 37°C and 5% CO<sub>2</sub>. After reaching a minimum confluence of 80%, the culture medium was removed from each well. The wells were then replenished with 200  $\mu$ L of test materials in triplicate: Alg-H, AMSC/Alg-H, or AMSC, which had been sectioned into minute fragments. The treated cells were incubated for an additional 48 hours under the same conditions. Cell viability was assessed using the MTT Assay Kit. A solution containing 9 mL of complete medium and 1 mL of MTT reagent was prepared in a 15 mL centrifuge tube and homogenized. 100  $\mu$ L of this mixture was added to each well, and the plates were incubated for 2–4 hours at 37°C and 5% CO<sub>2</sub> until formazan crystals developed. Following crystal formation, the solution was removed, and DMSO was added to halt the reaction. Absorbance was measured at 570 nm using a spectrophotometer. Cells treated only with culture medium served as a control, representing 100% viability. The viability of treated cells was calculated as a percentage relative to the control.<sup>29,30</sup>

## Cell Scratch Wound Assay

HaCaT cells were seeded onto 24-well plates at a density of 150,000 cells per well in 1000  $\mu$ L of culture medium. The plates were incubated at 37°C with 5% CO<sub>2</sub> for 24 hours or until the cells reached at least 80% confluence. Prior to the scratch assay, a horizontal line was drawn on the bottom of each well to serve as a reference point. Once a confluent monolayer was formed, a sterile yellow pipette tip was used to create a vertical scratch across the cell monolayer, intersecting the reference line. The old medium was carefully aspirated, and each well was gently washed with 1 mL of PBS (-) to remove cell debris. Following the scratch, the wells were treated with AMSC, Alg-H, or AMSC/Alg-H. The scratch closure was monitored by capturing images of the wounded area using an inverted microscope at 0, 24, and 48 hours post-scratch.<sup>31,32</sup>

## TGF- $\beta_1$ Level Measurement by ELISA

The concentration of TGF- $\beta_1$  in the supernatants of AMSC and AMSC/Alg-H cultures was quantified using a commercially available sandwich ELISA kit (product number RAB0460 and lot number 0426I0188). All procedures were performed according to the manufacturer's instructions. Briefly, 100  $\mu$ L of standards or samples were added to designated wells of the pre-coated microplate and incubated for 2.5 hours at room temperature or overnight at 4°C. The plate was then washed four times with 300  $\mu$ L of 1X Wash Solution using an automated plate washer. After the final wash, residual buffer was removed by aspiration, and the plate was inverted and blotted on lint-free paper towels. Subsequently, 100  $\mu$ L of biotinylated detection antibody (1x concentration) was added to each well and incubated for 1 hour at room temperature with gentle orbital shaking (100 rpm). Following another wash cycle, 100  $\mu$ L of Streptavidin-HRP conjugate was dispensed into each well, and the plate was sealed and incubated for 45 minutes at room temperature with mild agitation (100 rpm). After washing, 100  $\mu$ L of TMB Substrate Solution was added to each well and incubated for 30 minutes at room temperature in the dark. The enzymatic reaction was terminated by adding 50  $\mu$ L of Stop Solution (2N H<sub>2</sub>SO<sub>4</sub>) to each well. The optical density was immediately measured at 450 nm with wavelength correction set to 570 nm using a microplate spectrophotometer (model and manufacturer). TGF- $\beta_1$  concentrations were calculated using a four-parameter logistic regression curve fit of the standard values. The assay sensitivity and dynamic range should be stated, along with any sample dilutions performed.

## Statistical Analysis

The data are presented as average values along with the standard deviation. Statistical significance between groups was determined using one-way analysis of variance (ANOVA) and unpaired *t*-test, *p*-values < 0.05 were considered significant using GraphPad Prism 8.4.0.

# Results

## Morphology Studies

Cryo-electron microscopy (cryo-EM) is an effective method for examining biological samples such as stem cells. Cryo-EM has become the latest technological innovation in biological morphological observations, observation of molecules, and massive cells at certain atomic resolutions.<sup>33</sup>

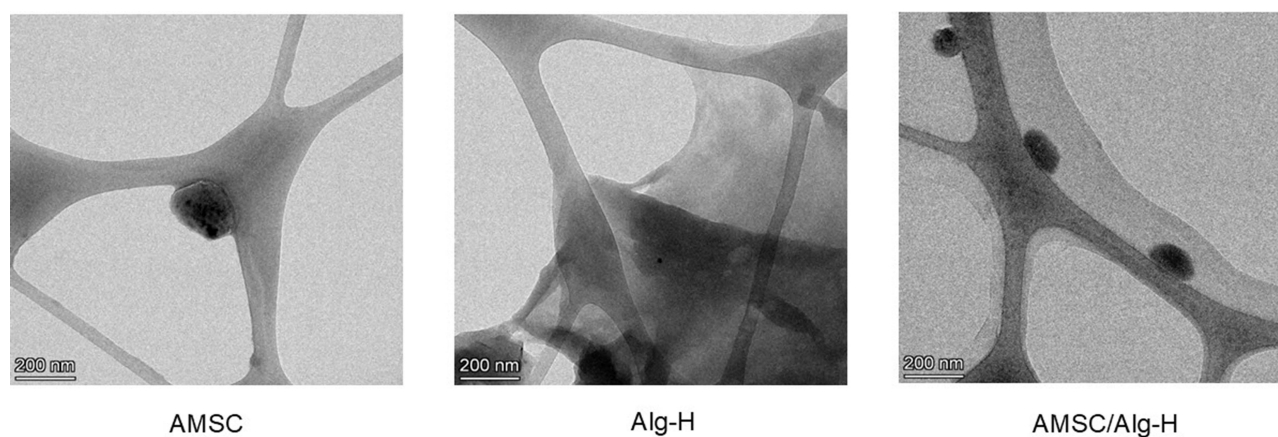


**Figure 1** Cryo-EM images of AMSC/Alg-H in magnification 45000x.

The research findings depicted in the image indicate the following. AMSC can be effectively observed. The Alg-H base resembled soft cotton material covering the cryo-EM lesion. The AMSC hydrogel consisted of AMSCs coated with a hydrogel substance that adhered to the cryo-EM lesion. Microscopic examination showed that AMSCs could maintain their morphology when encapsulated in Alg-H. Alg-H creates a suitable microenvironment for AMSCs, facilitating nutrients that are essential for maintaining AMSC viability.<sup>34,35</sup> Thus, the results are consistent with the creation of AMSC/Alg-H (Figure 1).

## Fourier-Transform Infrared Spectroscopy Analysis (FTIR)

The test sample was a combination of alginate,  $\text{CaCl}_2$ , and AMSC; therefore, the FTIR absorption pattern of the test sample had all the characteristics of alginate,  $\text{CaCl}_2$ , and AMSC (Table 2 and Figure 2). The modification in the FTIR spectrum arises from the interaction among sodium alginate,  $\text{CaCl}_2$ , and AMSC, resulting in the creation of a novel cross-linked structure, as evidenced by the alterations in the distinctive peaks of the FTIR spectrum.<sup>36,37</sup>

**Table 2** FT-IR Functional Group

Name of Sample	Characteristic Functional Group/Assignment	Wavenumber ( $\text{Cm}^{-1}$ )
AMSC	N-H stretching of proteins	3280–3300
	Amide I band ( $\text{C=O}$ stretching)	1640–1690
Alg-H	Hydroxyl group ( $-\text{OH}$ )	3200–3550
	Carbonyl group ( $\text{C=O}$ )	1600–1700
	C-O bond vibrations in the carboxylate group ( $-\text{COO}^-$ )	1410–1450
	Vibration of $\text{Ca}^{2+}$ ion with carboxylate group ( $-\text{COO}^-$ )	600–700
AMSC/Alg-H	Hydroxyl group ( $-\text{OH}$ )	3200–3550
	Triple bond (alkyne, $\text{C}\equiv\text{C}$ )	2100–2260
	Carbonyl group ( $\text{C=O}$ )	1600–1700
	C–O–C bond	1000–1150
	Vibration of $\text{Ca}^{2+}$ ion with carboxylate group ( $-\text{COO}^-$ )	600–700



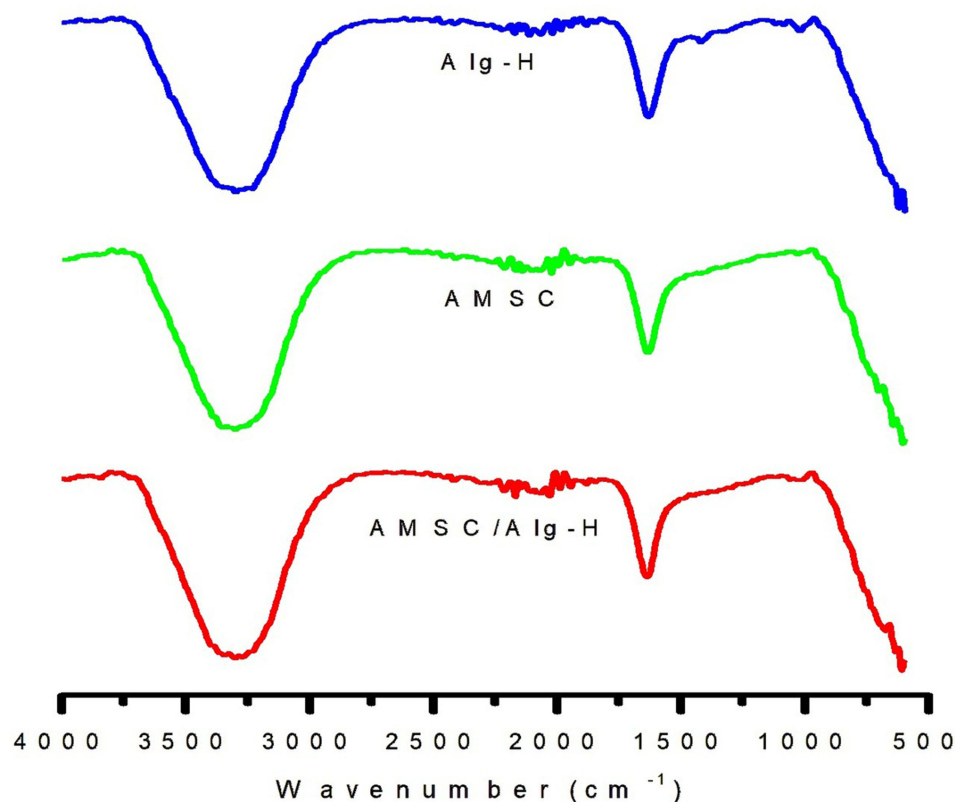


**Figure 2** Spectroscopy analysis by FTIR of AMSC/Alg-H.

## Differential Scanning Calorimetry Analysis (DSC)

The AMSC control shows an endothermic thermogram peak at 127.31°C, the Alg-H base exhibits an endothermic peak at 130.41 °C, and the AMSC/Alg-H preparation displays an endothermic peak at 128.64 °C. The creation of AMSC/Alg-H has a temperature that is 2°C lower, specifically 128.64°C, compared to the Alg-H base (Figure 3). This demonstrates a cross-link interaction of Alg-H that encapsulates AMSC. This data is additionally confirmed by FTIR analysis.

## Cytotoxicity Studies

The 3-(4,5-dimethylthiazol-2-yl)-2,5-diphenyltetrazolium bromide (MTT) assay was used to determine the viability and proliferation of cells, including amniotic membrane stem cells (AMSCs). Based on statistical by one way analysis of variance ( $p < 0.05$ ), AMSC/Alg-H and Alg-H were not significant, indicating that they were not toxic to HaCaT cells. HaCaT cells were still able to maintain their viability even after treatment with AMSC/Alg-H and Alg-H (Figure 4).

## Cell Scratch Wound Assay

The scratch wound test showed that HaCaT cell cultures treated with AMSC and AMSC/Alg-H showed the statistical by one way analysis of variance ( $p < 0.05$ ) for 0 h, AMSC was significantly with Alg-H and AMSC/Alg-H. After 24 h, AMSC was significantly with control and AMSC/ Alg-H, the percentage of wound closure was 100% at AMSC/Alg-H. The results demonstrate that wounds treated with AMSC/Alg-H healed more rapidly than other treatments. Microscopic observation revealed enhanced cell migration in the AMSC/Alg-H group, leading to complete wound closure within 24 hours. This finding suggests that AMSC/Alg-H has the potential to accelerate the wound healing process significantly (Figures 5 and 6).

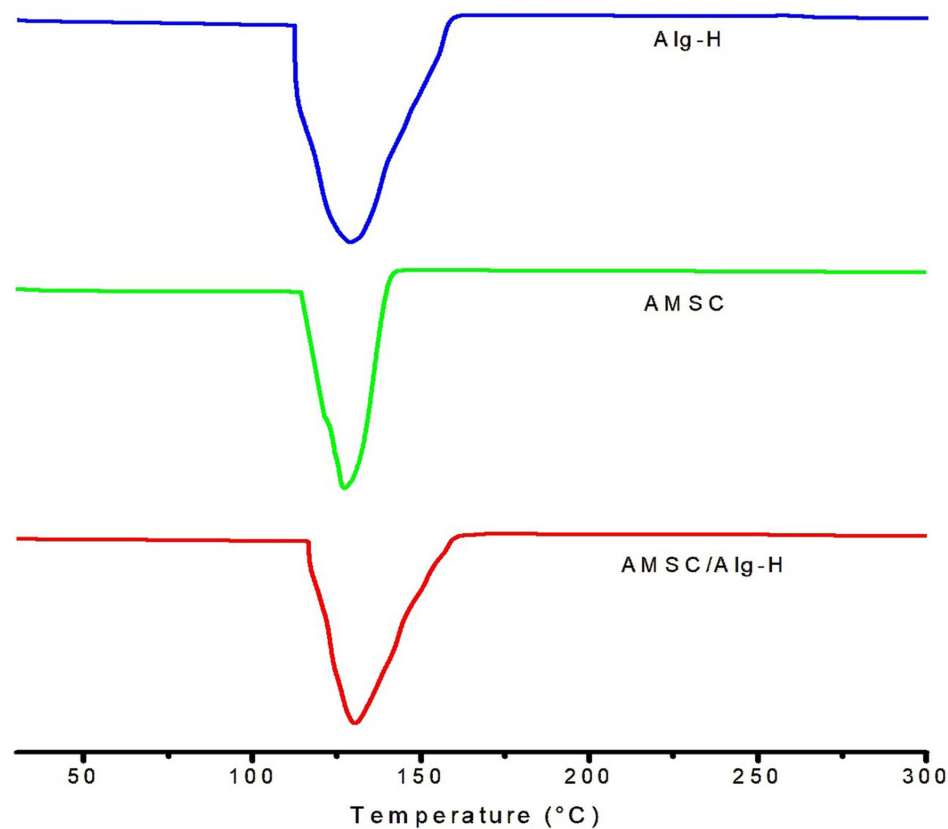


**Figure 3** Thermal analysis by DSC of AMSC/Alg-H.

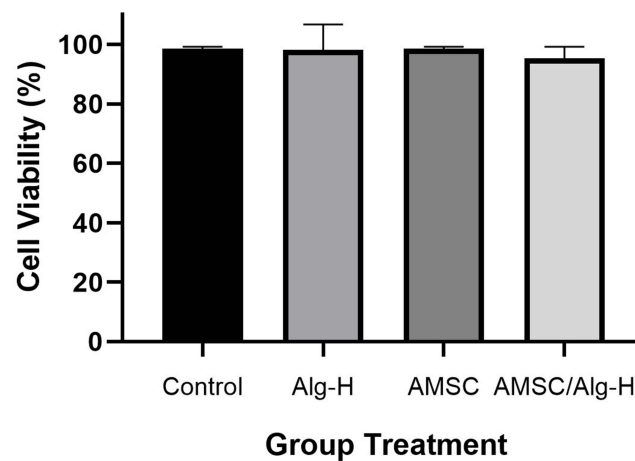


**Figure 4** HaCaT cell viability percentage of AMSC/Alg-H. Each value represents the mean  $\pm$  SD of three independent experiments performed in triplicate are presented. P values obtained by one way analysis of variance  $p < 0.05$ .

### TGF- $\beta_1$ Level Measurement Test

Transforming Growth Factor-beta 1 (TGF- $\beta_1$ ) is a cytokine that is important in various cellular processes, including cell proliferation, differentiation, and tissue repair.<sup>38</sup> Its detection and quantification of TGF- $\beta_1$  levels is essential for understanding the function of TGF- $\beta_1$  in physiological and pathological processes. TGF- $\beta_1$  levels in biological samples can be detected using Enzyme-Linked Immunosorbent Assay.<sup>39</sup>

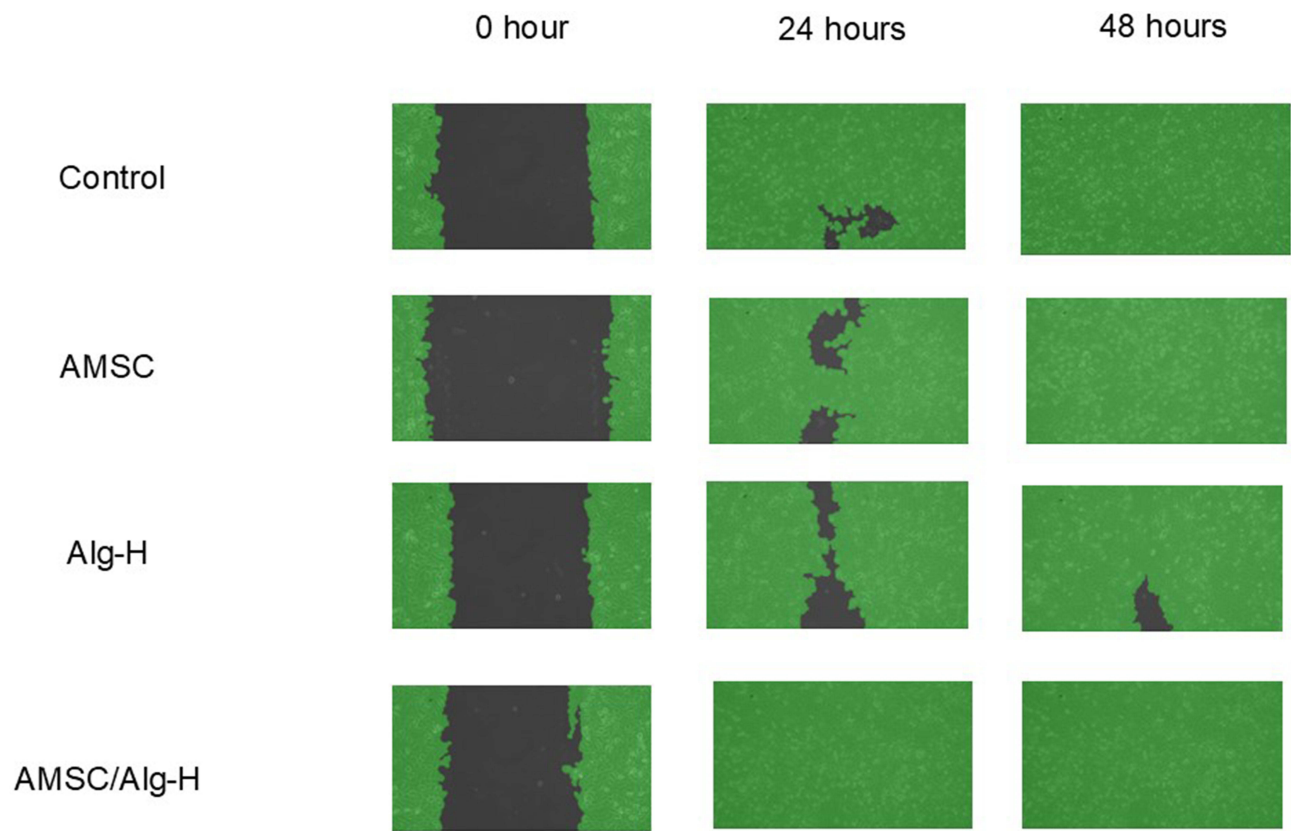


**Figure 5** Microscopic follow-up in vitro wound dressing process in presence of wound closure on scratch assay of AMSC/Alg-H.

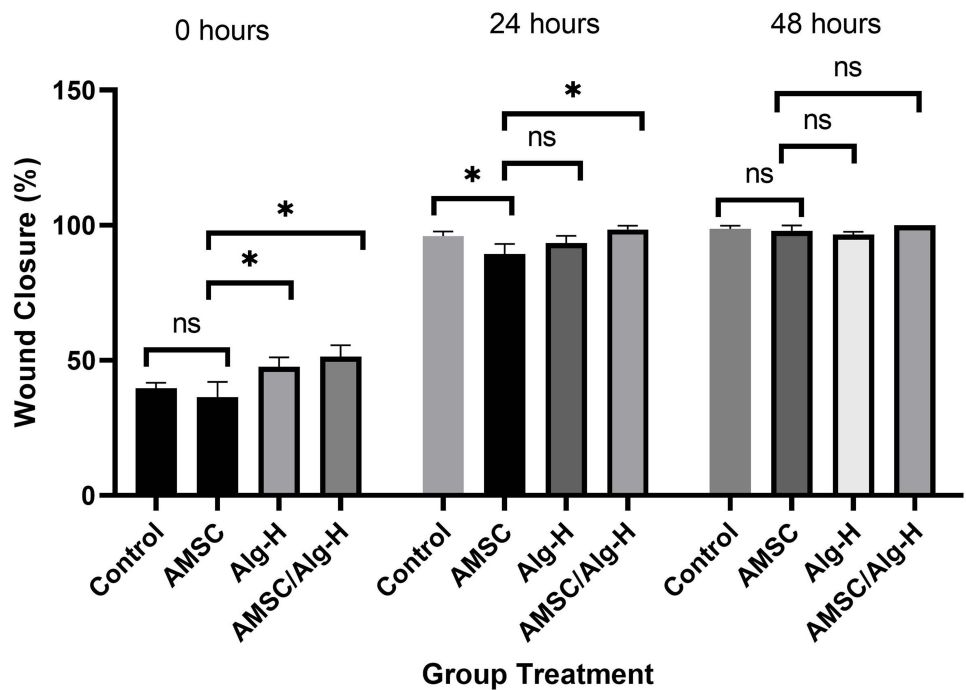


**Figure 6** HaCaT Cell scratch assay AMSC/Alg-H. Each value represents the mean  $\pm$  SD of three independent experiments performed in triplicate are presented. The data showed significant differences between the AMSC group and the Alg-H group as well as the AMSC group and the AMSC/Alg-H group at 0 hour, and between the control group and the AMSC group as well as the AMSC group and the AMSC/Alg-H group at 24 hours obtained by one way analysis of variance (\* $p < 0.05$ ).



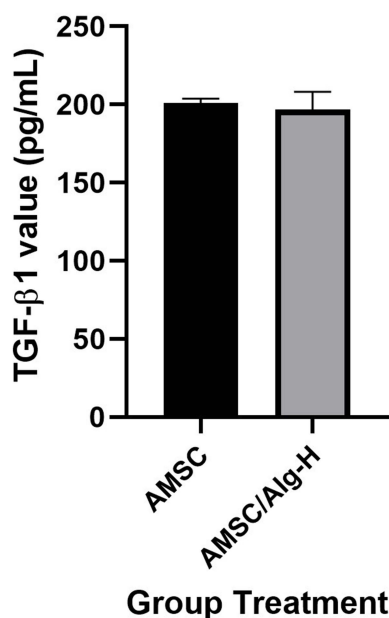


**Figure 7** TGF-β1 value (pg/mL) of AMSC/Alg-H. Each value represents the mean  $\pm$  SD of three independent experiments performed in triplicate are presented. P value obtained by unpaired *t*-test of  $p < 0.05$ .

Statistical analysis unpaired *t*-test ( $p < 0.05$ ) showed that the levels of TGF-β1 in AMSC and AMSCs/Alg-H were not significantly different. Thus, AMSC activity was not reduced when hydrogel preparations were made. Alg-H has properties comparable to those of AMSC; therefore, it can be used as a carrier in AMSC delivery (Figure 7).

## Discussion

Amniotic membranes have a significant effect on stem cell movement during wound healing. Other studies have shown that amniotic membranes can improve cell migration under controlled laboratory settings. AMSCs exhibit anti-inflammatory properties, reducing chronic wound inflammation by promoting cell migration and proliferation by enhancing keratinocyte activity, which is essential for effective re-epithelialization. The interaction between AMSCs and keratinocytes enhances proliferation and migration, thereby facilitating wound closure.<sup>40</sup> AMSCs enhance angiogenesis that supplies nutrients and oxygen to tissues in the healing process. AMSCs facilitate microvascular development and attract progenitor cells to the wound area, thereby accelerating tissue regeneration.<sup>10,40</sup> The results of a meta-analysis study showed that AMSC therapy significantly improved wound healing rates through mechanisms including increased angiogenesis and reduced inflammation.<sup>6</sup> The reduced immunogenicity of AMSCs makes them a good choice for allogeneic therapy. AMSCs show high proliferation rates and can be expanded in vitro while maintaining their original properties.<sup>7</sup>

Cryo-electron microscopy (cryo-EM) has been used to study protein structure variations in the heart using the internal environment of stem cells, namely, in human induced pluripotent stem cell-derived cardiomyocytes (hiPSC-CMs).<sup>41</sup> Based on the surface morphology results, it can be seen that the AMSC was encapsulated by an Alg/H base. Alg-H not only protects AMSCs but also facilitates their use in tissue engineering applications by providing a scaffold that mimics the extracellular matrix. This is important for applications in regenerative medicine where maintenance of cell function is critical.<sup>35</sup> This result is the same as that of previous research, which showed that the secretome was closed by physical interactions or electrostatic interactions with the polymer chains that formed the hydrogel system. This indicates that the biological components of the secretome cannot form chemical attachments with functional groups present in the matrix.<sup>42</sup> A recent study demonstrated that neural stem cells (NSCs) and mesenchymal stromal cells (MSCs) encapsulated with modified hyaluronic acid (HA) exhibited a loss of spherical morphology and extended processes when cultured on surfaces, indicating successful adherence and proliferation following encapsulation.<sup>43</sup> Human adipose-derived stem cells (hADSCs) encased in a P-SH-HA hydrogel, preserving an optimal milieu for stem cells.<sup>44</sup> Alginate hydrogel capsules designed for stem cell distribution exhibited both

circular and irregular pores on their surface, facilitating nutrient transport, which enabled the maintenance of viable mesenchymal stem cells (MSCs) within the capsules over time.<sup>15</sup> In this work, AMSC can be regulated within Alg-H; however, the biological components do not chemically interact with Alg-H. The interactions involved are predominantly physical or electrostatic, enabling AMSC to be encapsulated in Alg-H without directly altering its chemical composition. Consequently, the findings of this study indicate that AMSC encapsulated in Alg-H can grow efficiently throughout time.

The FTIR spectrum of sodium alginate exhibited significant alterations during cross-linking with  $\text{CaCl}_2$  in contrast to the spectrum of sodium alginate without cross-linking. The interaction between sodium alginate and  $\text{CaCl}_2$  resulted in the alteration and displacement of distinctive peaks in the FTIR spectrum. This indicates that there is an interaction between alginate and  $\text{CaCl}_2$ , which forms chemical cross-links. The carbonyl group is visible at the peak of the spectrum between  $1600\text{--}1700\text{ cm}^{-1}$ . Another spectral peak was detected at  $1410\text{--}1450\text{ cm}^{-1}$ , indicating the presence C-O bond vibrations in the carboxylate group ( $-\text{COO}-$ ). The changes observed in the FTIR spectrum were due to the interaction between sodium alginate and  $\text{CaCl}_2$ , which formed a cross-linked structure. This is evident from the observed changes in the characteristic peaks of the FTIR spectra.<sup>36,37</sup> The FTIR spectrum of AMSC revealed the presence of a hydroxyl group ( $-\text{OH}$ ), which was distinguished by a broad absorption peak at  $3200\text{--}3550\text{ cm}^{-1}$ , whereas the spectrum exhibited a carbonyl group ( $-\text{C}=\text{O}$ ) with an intensity of  $1600\text{--}1700\text{ cm}^{-1}$ , in addition to the presence of an alkyne bond.

Differential scanning calorimetry (DSC) is the predominant technique employed in the pharmaceutical industry to identify physical and chemical interactions, polymorphisms, solid transformations, and stability. The purpose of the DSC testing was to assess the impact of temperature on the formation of AMSC/Alg-H. This research demonstrates that interaction with AMSC leads to a reduction in the glass transition temperature. This is similar to the results of this research: the glass transition range in SC-PLLA is wider and the magnitude of change reduction from NA-PLLA to SC-PLLA, suggesting a reduction in the amount of amorphous phase present.<sup>45</sup> The ratio of the increase in heat capacity at the glass transition temperature is 0.17, indicating that a considerable portion of the chain segments lack the ability to change their shape, suggesting that the amorphous material is distinct from a typical molten polymer. The DSC thermogram of the Alg/H base exhibits an endothermic peak attributed to enthalpy changes, specifically the disruption of the carboxylate-calcium complex bonds.<sup>46</sup> Another study showed that the Tg value exhibited a rapid initial increase within the first 2 h, followed by a subsequent decline. The initial 2-hour period of cellulose manufacture showed a significant increase in Tg value due to increased chain proximity and higher glass transition temperature. Cross-linking processes increase the loss modulus and tand, with lignin concentration and hydrogen bonding enhancing the resolution.<sup>47</sup>

We carried out the MTT assay to evaluate cytotoxicity by measuring the metabolic activity of living cells, specifically the reduction of yellow tetrazolium salt (MTT), which the mitochondrial dehydrogenase enzyme in living cells converts into purple formazan crystals. The MTT assay results indicated that HaCaT cells exhibited elevated cell viability following treatment with AMSC/Alg-H and Alg-H. This aligns with microscopic studies demonstrating the viability of AMSCs in Alg-H, affirming that Alg-H facilitates AMSC proliferation. Research on adipose tissue-derived mesenchymal stem cells (MSCs) encased in sodium alginate hydrogel exhibited elevated cell viability for the entire culture duration. The MTT test was employed to evaluate metabolic activity at many time intervals. Despite an initial reduction in MTT absorbance post-encapsulation, later assessments demonstrated a rebound over time, signifying effective nutrition absorption within the capsules.<sup>48</sup> A separate study examined the extrusion technique for encapsulating hAdMSCs using alginate- $\text{CaCl}_2$ . Results demonstrated that whereas cultivated hAdMSCs survived for up to 7 days when encased in alginate beads, their viability was inferior to that of reference cultures without encapsulation. This indicates diminished metabolic activity resulting from the physical limitations imposed by the alginate matrix.<sup>15</sup> Another study used the MTT test on hAMS scaffold, and found that the hAMSC scaffold from alginate and gelatin is non-toxic, so it is safe to use to carry hAMSC, which supports the attachment, proliferation, and differentiation processes of hAMSC.<sup>49</sup>

Alg-H exhibits significant promise for wound healing owing to its biocompatibility, nontoxicity, and ready availability. It possesses the capacity to absorb excess liquid, maintain physical hydration, and reduce the quantity of bacteria.<sup>50</sup> Research suggests that it efficiently fills gaps in scratch tests and has the potential to be integrated with nanoparticles to enhance the healing process.<sup>17</sup> Alginate and extracellular matrix hydrogel patches, including mesenchymal stem cell secretomes, exhibit expedited skin wound healing.<sup>18</sup> In this study, AMSC/Alg-H unexpectedly attained a wound closure rate of 100% in a scratch assay conducted on HaCaT cells after 24 hours of exposure. This outcome was also congruent with the production of TGF- $\beta$ 1

generated by AMSC before and after formulation. This indicates that AMSC/Alg-H can maintain TGF- $\beta$ 1 levels appropriately to facilitate wound healing without inhibiting its physiological function. Maintaining stable levels of TGF- $\beta$ 1 in AMSC/Alg-H facilitates the migration of AMSCs within Alg-H to the injured location, promoting expedited and efficient repair. The study revealed that TGF- $\beta$ 1 enhanced the proliferation and expression of extracellular matrix genes in hUC-MSC, which are mesenchymal stem cells derived from the umbilical cord. TGF- $\beta$ 1 facilitates the healing of wounds by aiding stem cells.<sup>51</sup> Alternative formulations of mesenchymal stem cells did not disrupt the TGF- $\beta$ 1 signaling pathway, suggesting their potential to preserve TGF- $\beta$ 1 function and facilitate tissue repair.<sup>52</sup> TGF- $\beta$ 1 modulates the characteristics and functions of AMSCs. AMSCs release TGF- $\beta$ 1, leading to angiogenesis and tissue repair. TGF- $\beta$ 1 has been demonstrated to accelerate angiogenesis, enhance collagen and fibronectin synthesis, and promote the migration and proliferation of endothelial cells.<sup>53,54</sup> Another study demonstrated that alginate-CaCl<sub>2</sub> hydrogels exhibited favorable biocompatibility, low toxicity, and simplicity in gel production.<sup>55</sup> The observed result is likely attributable to the interconnectedness and permeability of the hydrogel matrix in AMSC/Alg-H biomaterials. According to prior research, this structure is thought to enhance the interaction with cells and tissues.<sup>42</sup> AMSCs secrete a range of growth factors, such as EGF and TGF- $\beta$ , to enhance the proliferation of keratinocytes, hence promoting wound healing and the regeneration of new epithelial tissue.<sup>40</sup> The combined effect of AMSC on Alg-H promotes cell growth and movement, therefore enhancing the process of wound healing.

## Conclusion

This research demonstrates that AMSC/Alg-H possesses significant potential to expedite wound healing. FT-IR, DSC, and Cryo-EM analyses of the AMSC/Alg-H demonstrated crosslinking inside the Alg-H hydrogel containing AMSC. Moreover, AMSC/Alg-H exhibits non-toxicity towards HaCaT cells and promotes wound closure, as demonstrated by the scratch wound assay and TGF- $\beta$ 1 levels, indicating that Alg-H is compatible with AMSC, thereby allowing the maintenance of AMSC levels within the Alg-H matrix to facilitate tissue regeneration. Future study on AMSC/Alg-H may be broadened to investigate alternative hydrogel materials for stem cell encapsulation and the therapy of degenerative illnesses by enhancing studies on the interactions among stem cells, hydrogels, and various growth factors.

## Acknowledgments

We extend our gratitude to the Rector of Universitas Padjadjaran for covering the Article Processing Charges (APC) and the Minister of Research and Higher Education, Republic of Indonesia, for their generous funding of this study.

## Disclosure

The authors declare no conflicts of interest in this work.

## References

1. Zhao RC. *Stem Cells: Basics and Clinical Translation.*; 2015. doi:10.1007/978-94-017-7273-0
2. Xu Y, Chen C, Hellwarth PB, Bao X. Biomaterials for stem cell engineering and biomanufacturing. *Bioact Mater.* 2019;4:366–379. doi:10.1016/j.bioactmat.2019.11.002
3. Zelen CM, Snyder RJ, Serena TE, Li WW. The use of human amnion/chorion membrane in the clinical setting for lower extremity repair: a review. *Clin Podiatr Med Surg.* 2015;32(1):135–146. doi:10.1016/j.cpm.2014.09.002
4. Pfister P, Wendel-Garcia PD, Meneau I, et al. Human amniotic membranes as an allogenic biological dressing for the treatment of burn wounds: protocol for a randomized-controlled study. *Contemp Clin Trials Commun.* 2023;36(July):101209. doi:10.1016/j.conctc.2023.101209
5. Prawoto AN, Dachlan I. Use of amniotic membrane for wound healing in burn injuries. *J Rekonstruksi Dan Estet.* 2022;7(2):64–71. doi:10.20473/jre.v7i2.36050
6. Bermani BF, Budi AS, Hutagalung MR. Efficacy of amniotic membrane-mesenchymal stem cell therapy for burn wounds: metaanalysis study. *J Rekonstruksi Dan Estet.* 2021;5(1):46. doi:10.20473/jre.v5i1.24326
7. Fitriani N, Wilar G, Narsa AC, Mohammed AFA, Wathoni N. Application of amniotic membrane in skin regeneration. *Pharmaceutics.* 2023;15(3):1–22. doi:10.3390/pharmaceutics15030748
8. Manuelpillai U, Moodley Y, Borlongan CV, Parolini O. Amniotic membrane and amniotic cells: potential therapeutic tools to combat tissue inflammation and fibrosis? *Placenta.* 2011;32:S320–S325. doi:10.1016/j.placenta.2011.04.010
9. V SBB, Khurshid SS, Fisher OZ, Khademosseini A, Peppas NA. Hydrogels in regenerative medicine. *Adv. Mater.* 2009;21(32–33):3307–3329. doi:10.1002/adma.200802106
10. Zhou Z, Xun J, Wu C, et al. Acceleration of burn wound healing by micronized amniotic membrane seeded with umbilical cord-derived mesenchymal stem cells. *Mater Today Bio.* 2023;20(May):100686. doi:10.1016/j.mtbio.2023.100686

11. Aghayan HR, Hosseini MS, Gholami M, et al. Mesenchymal stem cells' seeded amniotic membrane as a tissue-engineered dressing for wound healing. *Drug Deliv Transl Res.* **2022**;12(3):538–549. doi:10.1007/s13346-021-00952-3
12. Rajinikanth BS, Rajkumar DSR, K K, Vijayaragavan V. Chitosan-based biomaterial in wound healing: a review. *Cureus.* **2024**;16(2). doi:10.7759/cureus.55193
13. Zhang M, Zhao X. Alginate hydrogel dressings for advanced wound management. *Int J Biol Macromol.* **2020**;162:1414–1428. doi:10.1016/j.ijbiomac.2020.07.311
14. Pangiantuk A, Kaokaen P, Kunhorm P, Chaicharoenaudomrung N, Noisa P. 3D culture of alginate-hyaluronic acid hydrogel supports the stemness of human mesenchymal stem cells. *Sci Rep.* **2024**;14(1):1–14. doi:10.1038/s41598-024-54912-1
15. de Souza JB, Dos S RG, Rossi MC, et al. In vitro biological performance of alginate hydrogel capsules for stem cell delivery. *Front Bioeng Biotechnol.* **2021**;9:1–10. doi:10.3389/fbioe.2021.674581
16. Al-Hasani FJ, Hamad QA, Faheed NK. Enhancing the cell viability and antibacterial properties of alginate-based composite layer by adding active particulates. *Discov Appl Sci.* **2024**;6(2). doi:10.1007/s42452-024-05715-6
17. Froelich A, Jakubowska E, Wojtylko M, et al. Alginate-based materials loaded with nanoparticles in wound healing. *Pharmaceutics.* **2023**;15(4):1142. doi:10.3390/pharmaceutics15041142
18. Kwon JW, Savitri C, An B, Yang SW, Park K. Mesenchymal stem cell-derived secretomes-enriched alginate/ extracellular matrix hydrogel patch accelerates skin wound healing. *Biomater Res.* **2023**;27(1):1–20. doi:10.1186/s40824-023-00446-y
19. Mahheidari N, Kamalabadi-Farahani M, Nourani MR, et al. Biological study of skin wound treated with Alginate/Carboxymethyl cellulose/chorion membrane, diopside nanoparticles, and Botox A. *npj Regen Med.* **2024**;9(1). doi:10.1038/s41536-024-00354-2
20. Seifabadi ZS, Rezaei-Tazangi F, Azarbarz N, et al. Assessment of viability of wharton's jelly mesenchymal stem cells encapsulated in alginate scaffold by WST-8 assay kit. *Med J Cell Biol.* **2021**;9(1):42–47. doi:10.2478/acb-2021-0007
21. Wang S, Yang H, Tang Z, Long G, Huang W. 2015 wound dressing model of human umbilical cord.pdf. *Environmental Toxicology.* **2016**;31(12):2016. doi:10.1002/tox.22202
22. Thompson RF, Walker M, Siebert CA, Muench SP, Ranson NA. An introduction to sample preparation and imaging by cryo-electron microscopy for structural biology. *Methods.* **2016**;100(2016):3–15. doi:10.1016/j.ymeth.2016.02.017
23. Ruskin AI, Yu Z, Grigorieff N. Quantitative characterization of electron detectors for transmission electron microscopy. *J Struct Biol.* **2013**;184(3):385–393. doi:10.1016/j.jsb.2013.10.016
24. Nogales E. Biology Technique. *Nature methods.* **2016**;13(1):24–27. doi:10.1038/nmeth.3694
25. Coates J. Interpretation of infrared spectra, a practical approach. *Encycl Anal Chem.* **2000**;1–23. doi:10.1002/9780470027318.a5606
26. Stuart BH. *Infrared Spectroscopy. Fundamentals and Applications.* Vol 8; **2005**; doi:10.1002/0470011149
27. Meylina L, Muchtaridi M, Joni IM, Elamin KM, Wathoni N. Hyaluronic acid-coated chitosan nanoparticles as an active targeted carrier of alpha mangostin for breast cancer cells. *Polymers (Basel).* **2023**;15(4):1–13. doi:10.3390/polym15041025
28. Gallagher PK. Handbook of Thermal Analysis and Calorimetry. *Handb Therm Anal Calorim.* **2008**;5(C):ii. doi:10.1016/S1573-4374(13)60004-7
29. Boukamp P, Petrussevska RT, Breitkreutz D, Hornung J, Markham A, Fusenig NE. Normal keratinization in a spontaneously immortalized. *J Cell Biol.* **1988**;106(March):761–771. doi:10.1083/jcb.106.3.761
30. Alarifi S, Ali D, Verma A, Alakhtani S, Ali BA. Cytotoxicity and genotoxicity of copper oxide nanoparticles in human skin keratinocytes cells. *Int J Toxicol.* **2013**;32(4):296–307. doi:10.1177/1091581813487563
31. Jonkman JEN, Cathcart JA, Xu F, et al. Cell adhesion & migration an introduction to the wound healing assay using livecell microscopy an introduction to the wound healing assay using livecell microscopy. *Cell Adhes Migr.* **2014**;8(5):440–451. doi:10.4161/cam.36224
32. Felice F, Zambito Y, Belardinelli E, Fabiano A, Santoni T, Di Stefano R. Effect of different chitosan derivatives on in vitro scratch wound assay: a comparative study. *Int J Biol Macromol.* **2015**;76:236–241. doi:10.1016/j.ijbiomac.2015.02.041
33. Lucas BA. Visualizing everything, everywhere, all at once: cryo-EM and the new field of structureomics. *Curr Opin Struct Biol.* **2023**;81:102620. doi:10.1016/j.sbi.2023.102620
34. Al-Jaibaji O, Swioklo S, Gijbels K, Vaes B, Figueiredo FC, Connon CJ. Alginate encapsulated multipotent adult progenitor cells promote corneal stromal cell activation via release of soluble factors. *PLoS One.* **2018**;13(9):1–15. doi:10.1371/journal.pone.0202118
35. Bhattacharjee M, Ivirico JLE, Kan HM, et al. Preparation and characterization of amnion hydrogel and its synergistic effect with adipose derived stem cells towards IL1 $\beta$  activated chondrocytes. *Sci Rep.* **2020**;10(1):1–15. doi:10.1038/s41598-020-75921-w
36. Dmitrenko M, Zolotarev A, Ljamin V, et al. Novel membranes based on hydroxyethyl cellulose/sodium alginate for pervaporation dehydration of isopropanol. *Polymers (Basel).* **2021**;13(5):1–33. doi:10.3390/polym13050674
37. Savić Gajić IM, Savić IM, Svirčev Z. Preparation and characterization of alginate hydrogels with high water-retaining capacity. *Polymers.* **2023**;15(12):2592. doi:10.3390/polym15122592
38. Massagué J. TGF $\beta$  signalling in context. *Nat Rev Mol Cell Biol.* **2014**;13(10):616–630. doi:10.1038/nrm3434.TGF
39. Silva AKA, Richard C, Bessodes M, Scherman D, Merten OW. Growth factor delivery approaches in hydrogels. *Biomacromolecules.* **2009**;10(1):9–18. doi:10.1021/bm801103c
40. Ruiz-Cañada C, Bernabé-García Á, Liarte S, Rodríguez-Valiente M, Nicolás FJ. Chronic wound healing by amniotic membrane: TGF- $\beta$  and EGF signaling modulation in re-epithelialization. *Front Bioeng Biotechnol.* **2021**;9(July). doi:10.3389/fbioe.2021.689328
41. Woldeyes RA, Nishiga M, Vander Roest AS, et al. Cryo-electron tomography reveals the structural diversity of cardiac proteins in their cellular context. *bioRxiv Prepr Serv Biol.* **2023**. doi:10.1101/2023.10.26.564098
42. León-Campos MI, Rodríguez-Fuentes N, Claudio-Rizo JA, et al. Development and in vitro evaluation of a polymeric matrix of jellyfish collagen-human stem cell secretome-polyurethane for wound healing. *J Mater Sci.* **2023**;58(19):8047–8060. doi:10.1007/s10853-023-08522-3
43. Whitewolf J, Highley CB. Conformal encapsulation of mammalian stem cells using modified hyaluronic acid. *J Mater Chem B.* **2024**;12(29):7122–7134. doi:10.1039/d4tb00223g
44. Hassan W, Dong Y, Wang W. Encapsulation and 3D culture of human adipose-derived stem cells in an in-situ crosslinked hybrid hydrogel composed of PEG-based hyperbranched copolymer and hyaluronic acid. *Stem Cell Res Ther.* **2013**;4(2). doi:10.1186/scrt182
45. Mano JF, Gómez Ribelles JL, Alves NM, Salmerón Sanchez M. Glass transition dynamics and structural relaxation of PLLA studied by DSC: influence of crystallinity. *Polymer (Guildf).* **2005**;46((19 SPEC.ISS.)):8258–8265. doi:10.1016/j.polymer.2005.06.096

46. Abulateefeh SR, Taha MO. Enhanced drug encapsulation and extended release profiles of calcium-alginate nanoparticles by using tannic acid as a bridging cross-linking agent. *J Microencapsul.* **2015**;32(1):96–105. doi:10.3109/02652048.2014.985343
47. Kong W, Fu X, Yuan Y, Liu Z, Lei J. Preparation and thermal properties of crosslinked polyurethane/lauric acid composites as novel form stable phase change materials with a low degree of supercooling. *RSC Adv.* **2017**;7(47):29554–29562. doi:10.1039/c7ra04504b
48. Siburian M. The encapsulation effect on viability of mesenchymal stem cells. *J Farm Galen.* **2021**;7(1):1–9. doi:10.22487/j24428744.2021.v7.i1.15258
49. Hendrijantini N, Hartono P, Susilowati H, Hartono CK, Daniati RP, Brahmana F. Study of human amniotic membrane mesenchymal stem cells using gelatin and alginate as nontoxic scaffolds. *Recent Adv Biol Med.* **2019**;5:1. doi:10.18639/RABM.2019.877306
50. Ishfaq B, Khan IU, Khalid SH, Asghar S. Design and evaluation of sodium alginate-based hydrogel dressings containing *Betula utilis* extract for cutaneous wound healing. *Front Bioeng Biotechnol.* **2023**;11(January):1–11. doi:10.3389/fbioe.2023.1042077
51. Li D, Liu Q, Qi L, Dai X, Liu H, Wang Y. Low levels of TGF- $\beta$ 1 enhance human umbilical cord-derived mesenchymal stem cell fibronectin production and extend survival time in a rat model of lipopolysaccharide-induced acute lung injury. *Mol Med Rep.* **2016**;14(2):1681–1692. doi:10.3892/mmr.2016.5416
52. Li R, Wang R, Zhong S, et al. TGF- $\beta$ 1-overexpressing mesenchymal stem cells reciprocally regulate Th17/Treg cells by regulating the expression of IFN- $\gamma$ . *Open Life Sci.* **2021**;16(1):1193–1202. doi:10.1515/biol-2021-0118
53. Niknejad H, Deihim T, Solati-Hashjin M, Peirovi H. The effects of preservation procedures on amniotic membrane's ability to serve as a substrate for cultivation of endothelial cells. *Cryobiology.* **2011**;63(3):145–151. doi:10.1016/j.cryobiol.2011.08.003
54. Parolini O, Alviano F, Bagnara GP, et al. Concise review: isolation and characterization of cells from human term placenta: outcome of the first international workshop on placenta derived stem cells. *Stem Cells.* **2008**;26(2):300–311. doi:10.1634/stemcells.2007-0594
55. Lee KY, Mooney DJ. Alginate: properties and biomedical applications. *Prog Polym Sci.* **2012**;37(1):106–126. doi:10.1016/j.progpolymsci.2011.06.003

## Stem Cells and Cloning: Advances and Applications

### Publish your work in this journal

Stem Cells and Cloning: Advances and Applications is an international, peer-reviewed, open access journal. Areas of interest in established and emerging concepts in stem cell research include: Embryonic cell stems; Adult stem cells; Blastocysts; Cordblood stem cells; Stem cell transformation and culture; Therapeutic cloning; Umbilical cord blood and bone marrow cells; Laboratory, animal and human therapeutic studies; Philosophical and ethical issues related to stem cell research. This journal is indexed on CAS. The manuscript management system is completely online and includes a very quick and fair peer-review system, which is all easy to use. Visit <http://www.dovepress.com/testimonials.php> to read real quotes from published authors.

Submit your manuscript here: <https://www.dovepress.com/stem-cells-and-cloning-advances-and-applications-journal>

**Dovepress**  
Taylor & Francis Group